

Halogenation of Drugs Enhances Membrane Binding and Permeation

Grégori Gerebtzoff,^[a] Xiaochun Li-Blatter,^[a] Holger Fischer,^[b] Adrian Frentzel,^[c] and Anna Seelig*^[a]

Halogenation of drugs is commonly used to enhance membrane binding and permeation. We quantify the effect of replacing a hydrogen residue by a chlorine or a trifluoromethyl residue in position C-2 of promazine, perazine, and perphenazine analogues. Moreover, we investigate the influence of the position (C-6 and C-7) of residue CF₃ in benzopyranols. The twelve drugs are characterized by surface activity measurements, which yield the cross-sectional area, the air–water partition coefficient, and the critical micelle concentration. By using the first two parameters (A_D and K_{aw}) and the appropriate membrane packing density, the lipid–water partition coefficients, are calculated in excellent agreement

with the lipid–water partition coefficients measured by means of isothermal titration calorimetry for small unilamellar vesicles of 1-palmitoyl-2-oleoyl-sn-glycero-3-phosphocholine. Replacement of a hydrogen residue by a chlorine and a trifluoromethyl residue enhances the free energy of partitioning into the lipid membrane, on average by $\Delta G_{w} \approx -1.3$ or -4.5 kJ mol⁻¹, respectively, and the permeability coefficient by a factor of ~ 2 or ~ 9 , respectively. Despite exhibiting practically identical hydrophobicities, the two benzopyranol analogues differ in their permeability coefficients by almost an order of magnitude; this is due to their different cross-sectional areas at the air–water and lipid–water interfaces.

Introduction

Most drugs permeate biological membranes by passive diffusion. The extent of permeation depends, on one hand, on the properties of the membrane and, on the other, on those of the diffusing molecule. Membranes are highly organized, anisotropic systems that are nevertheless fluid enough to allow considerable translational, rotational, and flexing movements of the constituent lipid and protein molecules. Under physiological conditions, the lipid-bilayer membrane is in a liquid crystalline state and behaves like optically uniaxial crystals with the optical axis perpendicular to the surface of the membrane.^[1] This is in contrast to membrane-mimicking systems such as octanol or hexadecane, which are isotropic organic solvents. By using solid-state NMR techniques, a quantitative analysis of the molecular ordering and dynamics of a lipid bilayer has become possible with a segment-to-segment resolution. The packing density of the hydrocarbon chains is well described in terms of a statistical order profile. Membrane packing and ordering increase with the cholesterol content and decrease with increasing temperature or increasing fatty acyl chain unsaturation (for a review see ref. [2]).

The lateral packing density of a lipid bilayer can, alternatively, be assessed in comparison to the packing density of a lipid monolayer (for a review see ref. [3]). The packing density of planar bilayers consisting of the most abundant natural lipid, 1-palmitoyl-2-oleoyl-sn-glycero-3-phosphocholine, POPC, was determined as $\pi_M = 32$ mN m⁻¹ at ambient temperature.^[4] That of unilamellar lipid vesicles is somewhat lower and varies between $\pi_M = 25$ – 32 mN m⁻¹ depending on the size of the vesicle,^[5] while that of cholesterol-containing membranes such as erythrocyte membranes is higher ($\pi_M = 32$ – 35 mN m⁻¹).^[6] The membrane packing density influences binding^[7,8] and permeation^[9] of drugs in an exponential manner.

The properties of the drug with the strongest impact on membrane binding are hydrophobicity (which is suitably reflected by the air–water partition coefficient) and the cross-sectional area.^[9,10] Whereas partitioning into an isotropic organic solvent increases with the molecular volume,^[11] partitioning into an anisotropic lipid bilayer decreases exponentially with increasing cross-sectional area of the molecule.^[7,8,9] Drugs are generally weak bases or weak acids that are present in a charged as well as an uncharged form under physiological conditions. Charged and uncharged molecules can insert into the lipid–water interface; however, only a fraction of uncharged drugs can permeate a lipid membrane.

Strategies to enhance passive diffusion often consist of replacing a hydrogen residue by a chlorine or a trifluoromethyl residue. Despite the relatively high numbers of halogenated drugs on the market, little information is available on the quantitative effects of halogenation on drug binding to membranes and drug diffusion through membranes. We therefore quantify the influence of such replacements on the lipid–water partition coefficient, K_{w} and the permeability coefficient, P . We chose chlorinated and fluorinated phenothiazine analogues

[a] G. Gerebtzoff, X. Li-Blatter, Dr. A. Seelig
Biophysical Chemistry, Biozentrum, University of Basel
Klingelbergstrasse 70, 4056 Basel (Switzerland)
Fax: (+41) 61-267-21-89
E-mail: anna.seelig@unibas.ch

[b] Dr. H. Fischer
Present address: F. Hoffmann–La Roche Ltd.
Pharma Research, Molecular Properties
Grenzacherstrasse, 4070 Basel (Switzerland)

[c] Dr. A. Frentzel
Present Address: Mepha Pharma
Dornacherstrasse 14, 4147 Aesch (Switzerland)

(analogues of promazine, perazine, and perphenazine) to investigate the influence of the type of halogenation, and 6- and 7-trifluoromethyl benzopyranol to investigate the influence of the position of a $-\text{CF}_3$ group.^[12]

We characterized the drugs in terms of their cross-sectional area, A_D , their air–water partition coefficient, K_{aw} and their critical micelle concentration, CMC_D , which are all obtained by means of surface-activity measurements (SAMs).^[9,13] Using the first two parameters, A_D and K_{aw} we calculated K_w for membranes of different packing densities, π_M . This approach is validated by comparing the lipid–water partition coefficients predicted on the basis of surface-activity measurements with those determined by means of isothermal titration calorimetry, ITC.^[10]

The permeability coefficient, P , is then calculated by taking into account the lipid–water partition coefficient derived from surface-activity measurements, the ionization constant, and the $\text{p}K_a$ of the compound as outlined previously.^[14]

Experimental Section

Compounds: Promazine-HCl, triflupromazine-HCl, trifluoperazine-2HCl, and fluphenazine-HCl were obtained from Sigma–Aldrich, Steinheim, Germany. *cis*-Flupenthixol-2HCl, chlorpromazine-HCl, chlorperphenazine-HCl, 6-trifluoromethyl benzopyranol (6-trifluoromethyl-3,4-dihydro-4-(1,6-dihydro-1-methyl-6-oxo-3-pyridazinyl-oxo)-2,2-dimethyl-2H-1-benzopyran-3-ol) and 7-trifluoromethyl benzopyranol (7-trifluoromethyl-3,4-dihydro-4-(1,6-dihydro-1-methyl-6-oxo-3-pyridazinyl-oxo)-2,2-dimethyl-2H-1-benzopyran-3-ol) were kind gifts from Merck, Darmstadt, Germany. Perazine-dimaleate and chlorperazine-HCl were kindly provided by Jacek Wójcikowski, Institute of Pharmacology, Polish Academy of Science, Kraków, Poland, and by F. Hoffmann–La Roche Ltd., Basel, Switzerland, respectively.

Buffers: For SAMs and ITC, Tris/HCl buffer (50 mM), containing NaCl (114 mM) was used. SAMs were performed at ambient temperature ($T = 24 \pm 1^\circ\text{C}$), and ITC was measured at 37°C . Buffers were adjusted to pH 7.4 at the temperatures used for the respective measurements. For SAMs, stock solutions of drugs were prepared at concentrations of 10^{-4} – 10^{-2} M either in nanopure water with a resistance of 17 – $18 \text{ M}\Omega \text{ m}^{-1}$ or in methanol. For ITC drugs were dissolved in buffer solution.

For SAMs we either used a Teflon trough designed by Fromherz (Mayer Feintechnik, Göttingen Germany)^[15] with a filling volume of one compartment of 20 mL or a home-built Teflon trough (filling volume 3 mL). To maintain a constant humidity, the troughs were covered by a Plexiglas hood. The surface pressure, $\pi = \gamma_0 - \gamma$, where γ_0 is the surface tension of the pure buffer and γ the surface tension of the drug solution, was monitored with filter paper (Whatman No. 1) connected to a Wilhelmy balance. For drugs dissolved in methanol, the measured surface pressure was corrected for the intrinsic surface pressure of methanol.^[13] The total methanol concentration in the final drug solution was 10% (v/v). For the home-built trough, in which evaporation is not compensated for by an added volume as in the Fromherz trough, the surface pressure was corrected for the effects of evaporation and buoyancy.

The thermodynamics of drug adsorption at the air–water interface is described by the Gibbs adsorption isotherm:

$$d\pi = RT\Gamma d\ln C \quad (1)$$

Here C is the concentration of the amphiphile in the Teflon trough, RT is the thermal energy per mole, and Γ is the surface excess concentration defined as the inverse of the product of the Avogadro number, N_A , and the area requirement of the surface active molecule at the interface, A_S :

$$\Gamma = (N_A A_S)^{-1} \quad (2)$$

The surface excess concentration, Γ , increases with C up to a limiting value Γ_∞ . As long as Γ is constant, a plot of π versus $\log C$ yields a straight line. The area requirement of the compound, A_S , was evaluated from the quasilinear part, $d\pi/d\ln C$, of the Gibbs adsorption isotherm:

$$\Gamma_\infty = (1/RT) d\pi/d\ln C \quad (3)$$

For data analysis, we developed a program that selects the quasilinear part of the $\pi/\log C$ plot in an automatic and reproducible manner.

To evaluate the air–water partition coefficient, the Szyszkowski equation was used:

$$\pi = RT\Gamma_\infty \ln(K_{aw}C + 1) \quad (4)$$

This is an integral version of Equation (3) combined with a Langmuir adsorption isotherm. Combining Equations (2) and (4) allows evaluation of K_{aw} by calculating the slope of the linear regression line through data points corresponding to the quasilinear part of the π versus $\log C$ plot by using A_S , determined as described above:

$$K_{aw}C = e^{\pi A_S N_A / RT} - 1 \quad (5)$$

C is the equilibrium concentration of the drug, C_{eq} in bulk solution, which is defined as the total concentration, C_{tot} , minus the concentration of the drug adsorbed to the air–water interface, C_b :

$$C_{\text{eq}} = C_{\text{tot}} - C_b \quad (6)$$

C_b is the product of Γ and the surface area of the solution, A , per total volume, V ($C_b = \Gamma AV^{-1}$). C_b is negligibly small as long as K_{aw} is small ($< 10^6 \text{ M}^{-1}$) and is therefore generally neglected ($C_{\text{eq}} \sim C_{\text{tot}}$).^[9] In the present evaluation procedure, however, we correct for C_b ; this slightly influences the parameters of hydrophobic compounds, such as *trans*-flupenthixol.

Lipid–water partition coefficients determined from surface-activity measurements: Knowledge of the K_{aw} and the A_D of a drug allows estimation of K_w according to Equation (7):^[9]

$$K_w = K_{aw} e^{-\pi_M A_D / kT} \quad (7)$$

Here kT is the thermal energy, and π_M is the lipid packing density of the membrane. $K_w [\text{M}^{-1}]$ is defined as the quotient of mole fraction of drugs bound to the membrane, X_b , and the concentration of the drug in aqueous solution, $C_{\text{eq}} [\text{mol L}^{-1}]$:

$$K_w = X_b / C_{\text{eq}} \quad (8)$$

K_w can be transformed to the dimensionless partition coefficient, γ_{lw} defined as the quotient of the drug concentration in the membrane and the drug concentration in the aqueous phase, both

given in [mol L⁻¹]:

$$\gamma_{lw} = C_m/C_{eq} = C_1 \cdot K_{lw} \quad (9)$$

C_1 is the molar concentration of lipid ($C_1 = 1.05 \text{ mol L}^{-1}$) if the density of lipids is assumed to be $\rho = 0.8 \text{ kg L}^{-1}$ and the molecular weight is $M_w = 760.1 \text{ Da}$ (POPC).

Free energies: The free energy of self-association or micelle formation, ΔG_{mic} , the free energy of partitioning into the air–water interface, ΔG_{aw} and the free energy of partitioning into the lipid–water interface, ΔG_{lw} are obtained as follows:

$$\Delta G_{mic} = RT \ln (CMC_D/C_w) \quad (10)$$

$$\Delta G_{aw} = -RT \ln (C_w K_{aw}) \quad (11)$$

$$\Delta G_{lw} = -RT \ln (C_w K_{lw}) \quad (12)$$

where C_w is the molar concentration of water ($C_w = 55.5 \text{ mol L}^{-1}$ at $24 \pm 1 \text{ }^\circ\text{C}$ and $C_w = 55.3 \text{ mol L}^{-1}$ at $37 \text{ }^\circ\text{C}$).

Permeability coefficient: As outlined previously,^[14,16] P can be estimated on the basis of surface activity measurements. For a non-electrolyte P is proportional to the product of γ_{lw} and the diffusion coefficient, D :

$$P = \gamma_{lw} D / \Delta x \quad (13)$$

where Δx is the thickness of the membrane. The diffusion coefficient is defined as:

$$D = kT / (6\pi\eta r) \quad (14)$$

where kT is the thermal energy, η is the membrane viscosity, and r is the molecular radius, which is derived from A_D . For the following calculations, the membrane viscosity is assumed to be $\eta = 1$ poise and the membrane thickness, $\Delta x = 50 \text{ \AA}$.

The fraction of the nonionized form of a basic drug, f_A , that is present at a particular pH can be calculated as:

$$f_A = \frac{[A]}{[AH^+] + [A]} = (1 + 10^{pK_a - \text{pH}})^{-1} \quad (15)$$

where $[A]$ and $[AH^+]$ are the concentration of the uncharged and the ionized form of the drug, respectively. For the calculation of the permeability coefficients, we use the standard pK_a values corrected for temperature. The partition coefficient for the permeating species of a basic drug, γ_{lw}^* , is thus:

$$\gamma_{lw}^* = \gamma \cdot f_A \quad (16)$$

and the permeability coefficient is:

$$P = \gamma_{lw}^* D / \Delta x \quad (17)$$

Isothermal titration calorimetry: Drug partitioning into small unilamellar vesicles (SUVs) was measured by means of high-sensitivity ITC with a Microcal VP-ITC calorimeter (Microcal, Northampton, MA). A suspension of small unilamellar vesicles formed from 1-palmitoyl-2-oleoyl-*sn*-glycero-3-phosphocholine (POPC) ($C_1 = 30\text{--}35 \text{ } \mu\text{M}$) was injected in 3–10 μL aliquots into the drug solution in the calorimeter cell ($V_{cell} = 1.4037 \text{ mL}$) by using a Hamilton syringe

coupled with a stepping motor. For all drugs, injections gave rise to exothermic heats of reaction, produced by the partitioning of the drug into the membrane (for further details see refs. [10] and [17]).

For uncharged drugs, binding to the membrane is best described by a simple partition equilibrium:

$$K_{lw} = X_b / C_{eq} \quad (18)$$

For the charged cationic drugs used in the present investigation, this simple approach [Eq. (18)] is not adequate and yields concentration-dependent partition coefficients. This is due to the fact that partitioning of the drug into the electrically neutral lipid–water interface leads to a positive surface charge density, σ , (defined as total surface charge, Q_T per total membrane surface area, A_T) and, in turn, to a positive surface potential, Ψ . As a consequence, the lipid–water partition coefficient decreases with increasing concentration.^[18] A concentration-independent binding constant, K_{lw} , can either be obtained by plotting X_b/C_{eq} against C_{eq} and extrapolating to $C_{eq} = 0$, as shown previously for the binding of cationic peptides to POPC vesicles, or by applying the Gouy–Chapman theory.^[18]

Results

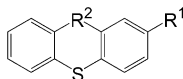
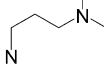
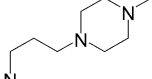
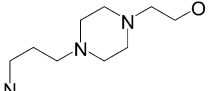
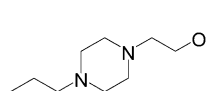
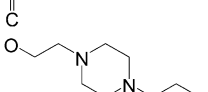
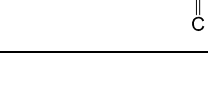
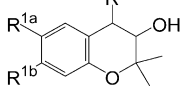
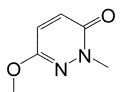
The compounds investigated are displayed in Table 1 A and B. The phenothiazine analogues, series A–C, as well as the benzopyranol analogues, series D, carry an uncharged or hydrophobic residue, R^1 , and a cationic or hydrophilic residue, R^2 , and are thus amphiphilic compounds. Series A–C represent promazine, perazine, and perphenazine analogues carrying a hydrogen atom, a chlorine atom, or a trifluoromethyl group as residue R^1 . Compounds in series D exhibit identical sum formulas but differ with respect to the position of the nonpolar $-\text{CF}_3$ group (R^{1a} and R^{1b}).

Surface activity measurements, SAMs

Injection of an amphiphilic drug into a monolayer trough filled with buffer is followed by partitioning of the drug between the aqueous phase and the air–water interface. Molecules in the air–water interface orient such that the hydrophilic residue, $-\text{R}^2$, remains immersed in the aqueous phase and the hydrophobic residue, $-\text{R}^1$, reaches into the air. The surface activity as a function of concentration ($\pi/\log C$ plot or Gibbs adsorption isotherm) was measured for all compounds at pH 7.4 and pH 8.0. The lower pH corresponds to the condition in aqueous bulk solution, and the higher pH reflects that close to an electrically neutral lipid membrane to which cationic drugs are bound and which therefore exhibits a positive surface potential, Ψ .^[5,19,20]

Cross-sectional areas, air–water partition coefficients, and critical micelle concentrations

Figure 1 shows the $\pi/\log C$ plots of the promazine and perazine analogues, series A and B, respectively. The slope of the quasilinear part of the Gibbs adsorption isotherm (solid line) yields the surface excess concentration, Γ_∞ [Eq. (3), below], and

Table 1. Analogues investigated.				
				
Series	Name	R ¹	R ²	
A	promazine	H		
	chlorpromazine	Cl		
	triflupromazine	CF ₃		
B	perazine	H		
	chlorperazine	Cl		
	trifluoperazine	CF ₃		
C	chlorperphenazine	Cl		
	fluphenazine	CF ₃		
		CF ₃		
	cis-flupenthixol	CF ₃		
	trans-flupenthixol	CF ₃		
				
Series	Name	R ^{1a}	R ^{1b}	R ²
D	6-(trifluoromethyl)benzopyranol	CF ₃	H	
	7-(trifluoromethyl)benzopyranol	H	CF ₃	

in turn the surface area requirement, A_s , of the drug molecule at the air–water interface [Eq. (2), below]. The intersection of the linear slope and the solid line drawn through the points of constant surface pressure at high concentrations is defined as the critical micelle concentration of the drug, CMC_D . Due to a comparatively low amphiphilicity (see Discussion) and a concomitant high tendency to aggregate at higher pH values, chlorpromazine could only be measured up to pH 7.8.

Figure 2A shows the $\pi/\log C$ plots of triflupromazine as a function of the pH. At high pH the compounds are only partially charged and therefore partition into the air–water interface even at low concentrations ($C < 10^{-6}$ M). The lower the pH of the solution, the lower is the air–water partition coefficient, K_{aw} , the flatter the slope of the $\pi/\log C$ plot and the larger the area requirement of the molecule at the air–water interface, A_s . The pH dependence of the surface area requirement, A_s (■) and the critical micelle concentration, CMC_D (Δ) for triflupromazine are summarized in Figure 2B. At low pH values where the drug is fully protonated, the area requirement at the interface, A_s , is large due to charge-repulsion effects,^[9] but decreases with increasing pH. For promazine (not shown) and triflupromazine (Figure 2B), the minimum area would, in principle,

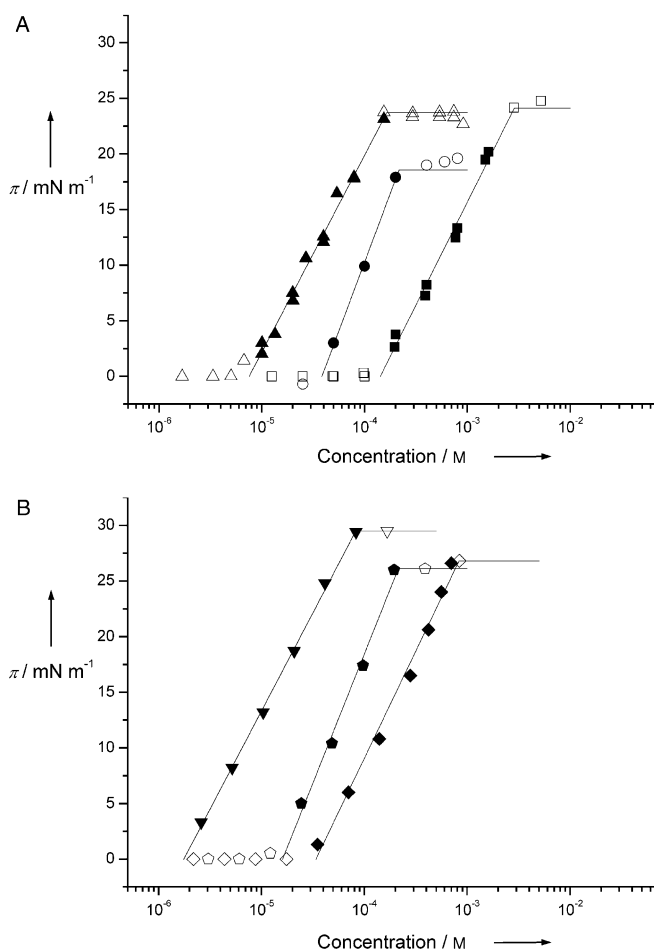


Figure 1. $\pi/\log C$ plots of promazine (series A) and perazine (series B) analogues. Solid symbols indicate the quasilinear part of the Gibbs adsorption isotherm. The corresponding slope is shown as a solid line. A) Promazine (squares), chlorpromazine (circles), and triflupromazine (triangles). The $\pi/\log C$ plots of promazine and triflupromazine consist of two independent measurements. B) Perazine (lozenges), chlorperazine (pentagons), and trifluoperazine (triangles). Measurements were performed at pH 8.0 (50 mM Tris/HCl containing 114 mM NaCl).

be reached close to pH 8.5. However, these drugs tend to form small micelles or aggregates, even below the apparent CMC_D at $pH > 7.5$. This can lead to a decrease in the slope of the Gibbs adsorption isotherm and, in turn, to a small apparent increase in area as seen in Figure 2B. Therefore, for the highly charged compounds promazine and triflupromazine, we used the extrapolated minimal values at pH 8.5 for the following calculations.

For most cationic drugs, however, the surface area requirement, A_s , measured at pH 8.0 corresponds well to the minimum area and thus reflects the cross-sectional area, A_{Dr} , of a drug as shown previously.^[9] Table 2 summarizes A_s , assumed to correspond to A_{Dr} , the corresponding K_{aw} and CMC_D .

Figure 2C shows the free energy of self association, ΔG_{mic} (<) [Eq. (12)] in comparison to the free energy of partitioning into the air–water interface, ΔG_{aw} (■) [Equation (10)] for triflupromazine. The difference between ΔG_{aw} and ΔG_{mic} was defined as the amphiphilicity, $\Delta\Delta G_{amr}$, of the compound:^[9]

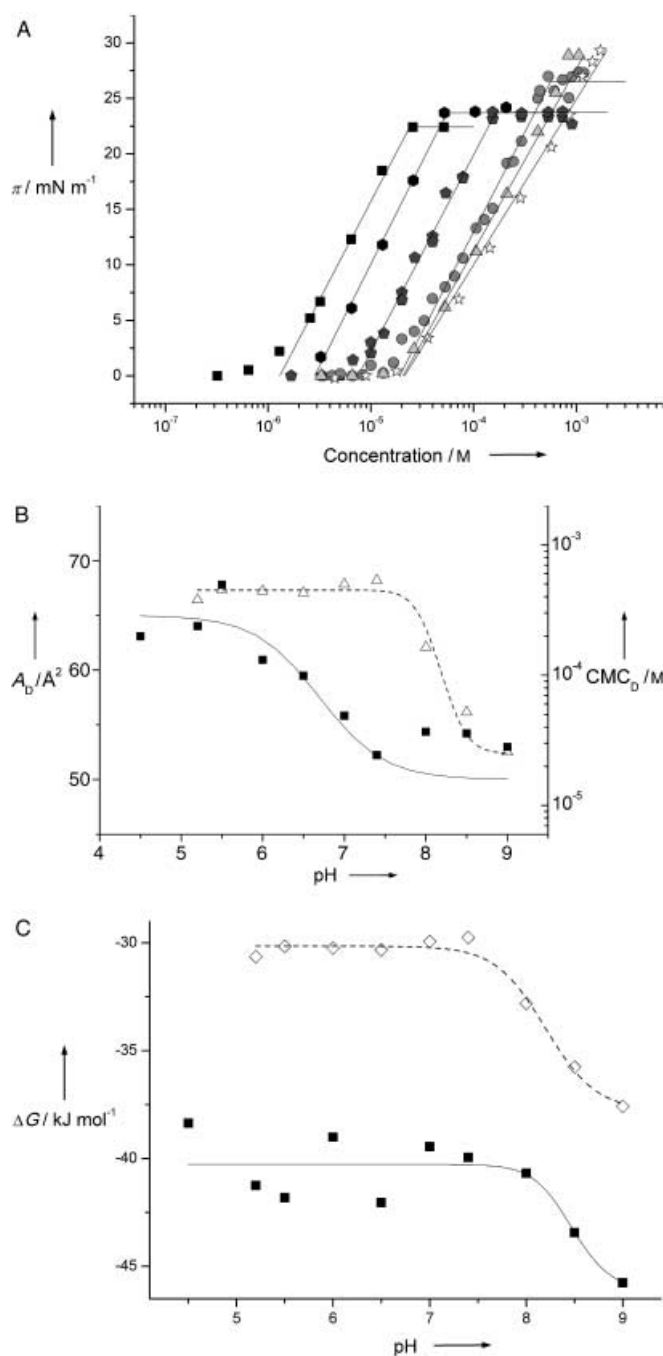


Figure 2. Surface-activity measurements of triflupromazine as a function of pH. A) $\pi/\log C$ plots at pH 4.5 (stars), pH 6.0 (triangles), pH 7.4 (circles), pH 8.0 (pentagons), pH 8.5 (hexagons), and pH 9.0 (squares). B) Cross-sectional area (squares), and critical micelle concentration (triangles). C) Free energy of partitioning into the air–water interface, ΔG_{aw} (squares), and free energy of micelle formation, ΔG_{mic} (diamonds). The solid and dashed lines in B and C are sigmoidal fits to the data.

$$\Delta G_{aw} - \Delta G_{mic} = \Delta \Delta G_{am} \quad (19)$$

As seen in Figure 2C, the amphiphilicity of triflupromazine is largest at low pH.

Figure 3A displays the $\pi/\log C$ plots of 6- and 7-trifluoromethyl benzopyranol at pH 8.0. The two compounds differ distinctly with respect to the slopes of the quasilinear part of the

Gibbs adsorption isotherms and thus with respect to the cross-sectional areas, A_D , as seen in Table 2. Moreover, they differ with respect to their amphiphilicity, 7-trifluoromethyl benzopyranol ($\Delta \Delta G_{am} = -7.73 \text{ kJ mol}^{-1}$) is more amphiphilic than 6-trifluoromethyl benzopyranol ($\Delta \Delta G_{am} = -6.94 \text{ kJ mol}^{-1}$). This can be rationalized by calculating the sum of the vectors of amphiphilicity. These were calculated for a set of multiple conformers from which the conformer with the highest amphiphilic moment was selected.^[21] Figure 3B displays the calculated vectors of amphiphilicity,^[21] which are $\Delta \Delta G_{am} = -7.41$ and $-5.54 \text{ kJ mol}^{-1}$, respectively; this is in reasonable agreement with the measured amphiphilicities.^[9] Here the amphiphilicities are given for $T = 24^\circ \text{C}$.

Lipid–water partition coefficient

Knowledge of K_{aw} and A_D allows calculation of K_{lw} for membranes with a specific π_M according to Equation (7). For the present calculations we used $\pi_M = 27$ and 35 mN m^{-1} , for SUVs formed from POPC at 37°C ^[5,10] or cholesterol-containing natural membranes, respectively.^[6] Calculated lipid–water partition coefficients are summarized in Table 2. For comparison, K_{lw} 's of the phenothiazine analogues were also measured by means of ITC. As an example, the titration of a fluphenazine solution by SUVs formed from POPC is displayed in Figure 4A. The titration of all phenothiazines gave rise to exothermic titration patterns. With increasing lipid concentration, the free-drug concentration in the measuring cell and the heat flow decreased concomitantly. Figure 4B shows the heats of reaction, h_i , obtained by integration of the heat-flow peaks. The molar binding enthalpy ΔH_{exp}^0 was determined directly from the cumulative heat release.^[10,17]

Permeability coefficients

The permeability coefficients, P , were calculated according to Equation (17) for membranes with lateral packing densities of $\pi = 27$ and 35 mN m^{-1} by using the pK_a values of the drugs at 37°C .^[23] The data are summarized in Table 2.

Discussion

In the following, we discuss the effects of drug halogenation on a drug's ability to permeate membranes. We place special emphasis on analyzing the difference between replacing a hydrogen residue by a chlorine or a trifluoromethyl residue in phenothiazine analogues (Table 1 series A–C). Moreover, we analyze the influence of the position of a $-\text{CF}_3$ residue in benzopyranol analogues (series D). To this purpose, we characterized twelve different drugs by means of SAMs. Measurements of the surface pressure as a function of concentration (Gibbs adsorption isotherms) yield i) the cross-sectional area, A_D , of the molecule when it is oriented in the amphiphilic gradient of the air–water interface or the lipid–water interface, ii) K_{aw} which mainly reflects the hydrophobicity of the compound, and iii) CMC_D , which reflects the tendency of the compound to

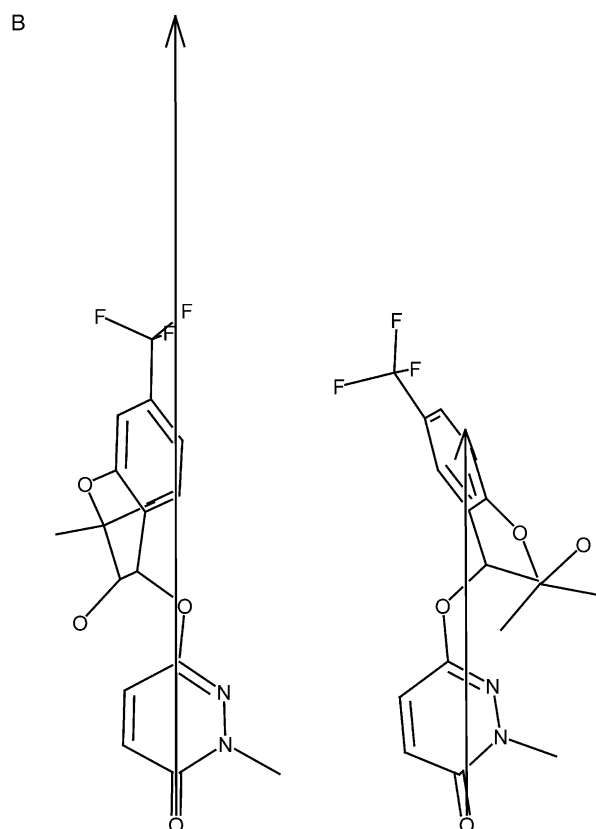
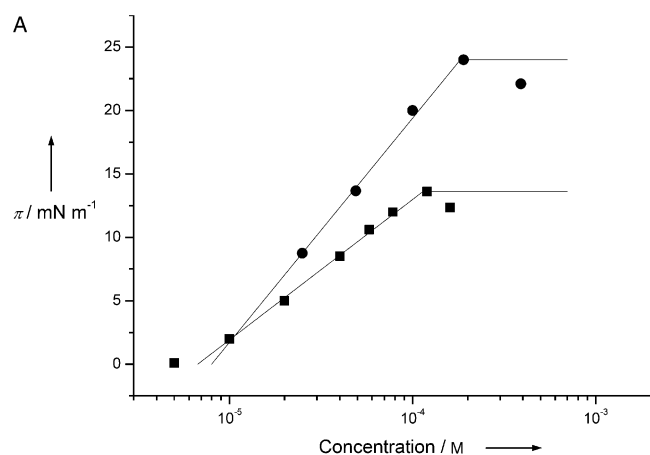


Figure 3. A) Gibbs adsorption isotherms ($\pi/\log C$ plots) of 6-trifluoromethyl benzopyranol (squares) and 7-trifluoromethyl benzopyranol (circles) measured at pH 8.0 (50 mM Tris/HCl containing 114 mM NaCl). B) Calculation of the vector of amphiphilicity for 6- (right) and 7-trifluoromethyl benzopyranol (left) with the program CAFCA.^[21] The vector addition starts from the most hydrophilic residue (the oxygen atom of the pyridazin-3-one moiety was taken as an initial point) and points towards the most hydrophobic region of the molecule. The direction of the vector indicates the most probable orientation of the molecule in the amphiphilic gradient of the air–water interface. Conformer selection was performed according to the procedure described previously.^[21] Briefly, vectors of amphiphilicity were calculated for a set of multiple conformers from which the conformer with the highest amphiphilic moment was selected.

self associate in solution. K_{lw} and P are calculated on the basis of the data obtained from SAMs as outlined previously.^[10,14]

The effect of halogenation is discussed on three levels: the first level deals with drugs in solution and at the air–water interface, which are characterized by the ionization constant,

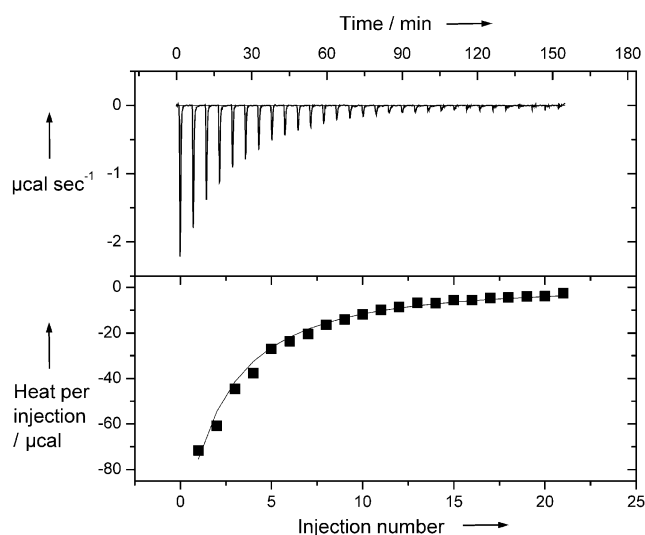


Figure 4. Isothermal titration calorimetry of fluphenazine. The fluphenazine solution (101.88 μM) was contained in the measuring cell of a calorimeter and SUVs (10.1 mM) were injected (4 μL at each injection). Measurements were performed in buffer solution (50 mM Tris, 114 mM NaCl) at pH 7.4 and a temperature of 37°C. Top: Titration curve. Bottom: Heats of reaction, h_r . The solid line is the theoretical binding isotherm calculated according to the Gouy–Chapman theory.

pK_a , the critical micelle concentration, and the air–water partition coefficient. The second level deals with the thermodynamics of interfacial membrane partitioning, and the third level with the kinetics of membrane permeation.

Drugs in solution and at the air–water interface

Ionization constants of the drugs in aqueous solution (standard values) are given in Table 2. For the promazine analogues, the pK_a values decrease with increasing electronegativity of residue R^1 in the order $\text{H} > \text{Cl} > \text{CF}_3$; this is in agreement with previous observations.^[22] For the perazine and perphenazine analogues this effect is less pronounced.

Apparent ionization constants depend on many factors such as temperature,^[23] the dielectric constant, ϵ_r , of the environment, and the association state of the drug.^[24] The pK_a values of a drug at the air–water interface and in a drug micelle differ from that of a drug in solution since neighboring charged groups influence each other.^[24] The ionization constant of a drug at the air–water interface under conditions in which only half of the air–water interface is occupied ($\Gamma = \Gamma_{\infty}/2$) is obtained from the pH dependence of ΔG_{aw} (Figure 2C). The ionization constant under conditions in which the air–water interface is fully occupied ($\Gamma = \Gamma_{\infty}$) is obtained from the pH dependence of surface area requirement, A_s (Figure 2B). For trifluopromazine the respective values are $pK_a(\Gamma_{\infty}/2) = 8.5$ and $pK_a(\Gamma_{\infty}) = 6.7$. From these two values it is possible to estimate the pK_a value of the monomer in solution as outlined previously.^[24] An intermediate value is obtained for the pH dependence of critical micelle concentration, CMC_D (Figure 2B and C) ($pK_a(\text{CMC}) = 8.2$). This is consistent with small, highly curved vesicles for which the splay of the head groups is larger than in a tightly packed

Table 2. Data obtained from surface-activity measurements and isothermal titration calorimetry.

Series	Compound	M_w (base) [g mol ⁻¹]	pK_a	pK_a 37°C	$A_D^{[a]}$ [Å ²]	K_{aw} [mM ⁻¹]	CMC_D [mM]	$\Delta\Delta G_{am}$ [kJ mol ⁻¹]	K_{wcalc} [mM ⁻¹] (27 mNm ⁻¹)	K_{wITC} [mM ⁻¹]	$D \times 10^8$ [cm ² s ⁻¹]	P [cm s ⁻¹] (27 mNm ⁻¹)	P [cm s ⁻¹] (35 mNm ⁻¹)
A	Promazine	284.42	9.42 ^[27]	9.1	42.0	15	2.86	-9.69	1.20	1.55 ^[10]	5.38	11	5
	Chlorpromazine	318.86	9.2 ^[28]	8.9	40.0	20	0.22	-3.78	1.61	2.34 ^[10]	6.36	26	12
	Triflupromazine	352.42	9.07 ^[29]	8.7	50.0	129	0.16	-7.88	5.52	5.10 ^[10]	5.34	102	40
B	Perazine	339.5	8.01 ^[30]	7.7	42.0	30	0.83	-8.32	2.14	2.20	5.53	184	84
	Chlorperazine	373.94	8.1 ^[31]	7.8	41.1	61	0.21	-6.60	4.53	4.53	6.28	367	170
	Trifluoperazine	407.5	8.08 ^[32]	7.8	57.4	609	0.08	-10.11	15.71	17.60 ^[10]	5.29	1088	368
C	Chlorperphenazine	403.97	7.9 ^[29]	7.6	50.3	105	0.11	-6.35	4.42	4.50	5.67	377	147
	Fluphenazine	437.52	8.1 ^[31]	7.8	55.4	520	0.10	-10.22	15.78	14.00	5.41	1038	390
	cis-flupenthixol	434.52	7.8 ^[33]	7.5	63.0	1081	0.05	-10.47	20.31	20.00 ^[10]	5.07	1633	503
	trans-flupenthixol	434.52	7.8 ^[33]	7.5	66.0	4504	0.032	-12.8	70.02	24.00	4.95	5503	1602
D	6-trifluoromethyl benzopyranol	370.11	2.61	2.4	85.4	138	0.12	-7.24	0.63		4.35	58	12
	7-trifluoromethyl benzopyranol	370.11	2.61	2.4	53.9	121	0.19	-8.07	4.04		5.48	465	1670

[a] For the highly charged molecules promazine and triflupromazine the minimum area, A_D , was extrapolated to pH 8.5. Data given represent average values from several measurements. Maximum error range is $\pm 5\%$. A_D is the cross-sectional area, CMC_D , the critical micelle concentration, and K_{aw} the air-water partition coefficient [Equation (5)]. K_w is the lipid-water partition coefficient which was either calculated according to Equation (7), K_{wcalc} or measured by means of isothermal titration calorimetry, K_{wITC} . D is the diffusion coefficient [Equation (14)], and P , the permeability coefficient [Equation (17)]. SAM and ITC were performed at $24 \pm 1^\circ\text{C}$ and 37°C , respectively. For simplicity all ΔG values were calculated at 37°C .

planar drug layer at the air-water interface but smaller than that at a half-occupied air-water interface ($\Gamma_{c/2}$).

Shifts of ionization constants to lower values are also observed if drugs insert into the lipid-water interface.

The cross-sectional areas of the phenothiazine analogues in series A-C vary between $A_D = 40$ and 58 \AA^2 . Only the flupenthixols exhibit slightly larger cross-sectional areas; this might be due to the rigidity of the double bond in residue R^2 . Replacement of a H atom by a Cl atom does not, on average, lead to a significant increase in A_D , in contrast to a replacement by a $-\text{CF}_3$ group, which leads to a measurable increase. The A_D ratios for the different analogues vary between $r = 1.0$ and $r = 1.4$ and are given in Table 3.

Measurement of the two analogues of series D, 6- and 7-trifluoromethyl benzopyranol, revealed an A_D ratio $r = 1.6$ (Table 3). The change in the cross-sectional area upon changing the position of the CF_3 group is thus due to a change in the orientation of the vector of amphiphilicity drawn from the most hydrophilic residue R^2 , immersed in aqueous solution ($\epsilon \sim 80$), to the most distant hydrophobic residue R^1 , reaching into the air ($\epsilon \sim 1$), as illustrated in Figure 3B.^[21] Since the dielectric constant of air is similar to that of lipids ($\epsilon \sim 2$), it can be assumed that the molecular orientation at the two interfaces is identical.

The air-water partition coefficient increases for compounds in series A-C in the order: $\text{H} < \text{Cl} < \text{CF}_3$ and reflects the increase in hydrophobicity of residues R^1 . Replacement of H by Cl or CF_3 leads, on average, to an increase in K_{aw} of a factor of approximately $r = 2$ or $r = 14$, respectively, or to an increase in the negative free energy of partitioning into the air-water interface of -1.5 or -6.6 kJ mol^{-1} , respectively. The effect of hal-

Table 3. Ratios, r , of cross-sectional areas, air-water partition coefficients, critical micelle concentrations, lipid-water partition coefficients (calculated from SAMs), and permeability coefficients for analogues with and without halogen residues.

Residue R^1	Series	rA_D	rK_{aw}	rK_w	rP (27 mNm ⁻¹)	rP (35 mNm ⁻¹)
Cl/H	A	1	1.34	1.3	2.40	2.50
	B	1	2.0	2.13	1.99	2.02
CF_3/H	A	1.25	8.62	4.48	9.56	8.24
	B	1.38	20.13	7.08	5.91	4.38
CF_3/Cl	A	1.25	6.45	2.85	3.98	3.30
	B	1.4	10.04	2.53	2.97	2.17
	C	1.1	4.93	3.25	2.92	2.65
CF_3 trans/cis	C	1.05	4.17	3.45	3.37	3.19
	D	1.59	1.15	0.45	0.12	0.07

ogenation is somewhat more pronounced in perazine than in promazine analogues. This may be due to the fact that the effect of charge still dominates in the latter analogues. The air-water partition coefficients of the two benzopyranol analogues in series D are practically identical.

The free energy of self-association or micelle formation, ΔG_{mic} is significantly enhanced by the replacement of a H by a Cl or a CF_3 residue. Surprisingly, at first, the difference between the two halogen residues is small.

The amphiphilicity, $\Delta\Delta G_{\text{amv}}$, which is the difference between the free energy of partitioning into the air–water interface, ΔG_{aw} and the free energy of micelle formation, ΔG_{mic} ^[9] increases with increasing charge of the compound at constant hydrophobicity or with increasing hydrophobicity at constant charge (Table 4). For the drugs under study $\Delta\Delta G_{\text{am}}$ increases in

Table 4. Difference in free energies of air–water partitioning, micelle formation or self-association, and membrane partitioning of analogues with and without halogen residues calculated from SAMs.

Residue R ¹	Series	ΔG_{aw} [kJ mol ⁻¹]	ΔG_{mic} [kJ mol ⁻¹]	ΔG_{lw} [kJ mol ⁻¹]
Cl/H	A	-0.75	-6.66	-0.75
	B	-1.79	-3.51	-1.94
CF ₃ /H	A	-5.55	-7.36	-3.93
	B	-7.74	-5.95	-5.14
CF ₃ /Cl	A	-4.81	-0.70	-3.18
	B	-5.95	-2.44	-3.20
CF ₃ <i>trans/cis</i>	C	-4.11	-0.24	-3.28
	C	-3.68	-1.35	-3.19
7-CF ₃ /6-CF ₃	D	-0.35	-1.18	-4.79

the order: Cl < H < CF₃. The comparatively low critical micelle concentrations and amphiphilicities of the chlorinated analogues in series A, B and C is most probably due to the relatively strong reduction in pK_a values combined with a negligibly small increase in hydrophobicity upon chlorination, and explains the comparatively high tendency of these analogues to aggregate in solution.

Interfacial membrane partitioning

The lipid–water partition coefficients were calculated according to Equation (7) by using the K_{aw} and A_{D} of the compound measured under conditions of minimal electrostatic repulsion for membranes with a packing density, $\pi_{\text{M}} = 27$ and 35 mN m⁻¹, corresponding to that of small unilamellar vesicles formed from POPC at physiological temperature and that of cholesterol-containing membranes, respectively. As seen in Table 2, the lipid–water partition coefficients calculated for a membrane packing density of $\pi_{\text{M}} = 27$ mN m⁻¹ are in excellent agreement with those measured for small unilamellar POPC vesicles by means of ITC.^[10] The lipid–water partition coefficients for the promazine analogues have also been measured by means of spectrophotometric techniques and are also in good agreement (if transformed to the same units).^[26]

The lipid–water partition coefficients of the compounds in series A–C increase in the order of residue R¹: H > Cl > CF₃. The exchange of a H to Cl or CF₃ leads on average to an increase in the negative free energy of membrane partitioning of $\Delta G_{\text{lw}} = -1.5$ or -4.5 kJ mol⁻¹, respectively. The dominant factor is the increase in hydrophobicity. For compounds in series D that exhibit similar hydrophobicities, the lipid–water partition coefficients are dominated by the different cross-sectional areas, A_{D} (Table 3).

Membrane permeation

On a third level, the kinetics of passive diffusion through the lipid membrane are calculated on the basis of simple Stokesian diffusion by using the parameters obtained from surface-activity measurements and taking into account the pK_a value of the drugs. For a replacement of H by a Cl or a CF₃ residue, the permeability coefficient, P , increases on average by a factor of approximately $r = 2$ or $r = 9$, respectively. The increase is again somewhat larger for promazine than for perazine analogues. Despite the differences between promazines and perazines, the increase in P upon replacement of Cl by CF₃ is rather constant for all three types of analogues (promazines, perazines, and perphenazines) and amounts to about $r = 3.5$ (Table 3). It is interesting to note that the two isomers, *cis*- and *trans*-flupenthixol, differ distinctly in their K_{aw} and K_{lw} as well as in P . Due to the relatively small cross-sectional areas of the above analogues, the packing density dependence of P is relatively small for the phenothiazine analogues. This is different for 7- and 6-trifluoromethyl benzopyranol, for which the ratios in permeability coefficients are $r = 0.12$ at the lower packing density investigated and only $r = 0.07$ at the higher.

Conclusion

A characterization of drugs by SAMs allows a detailed analysis of the effect of halogenation. The air–water and the lipid–water partition coefficients of promazine, perazine, and perphenazine analogues increase in the order, R¹: H < Cl < CF₃ due to the increase in hydrophobicity, despite a small increase in cross-sectional area. The permeability coefficient increases in the same order due to the increase in the lipid–water partition coefficient and the decrease in the pK_a values. For the small phenothiazine analogues, the packing density dependence of the permeability coefficient is rather small. The amphiphilicity of the halogenated analogues increases in the order R¹: Cl < H < CH₃; this explains the higher tendency of the chlorinated analogues to aggregate. As shown for benzopyranols, the position of a trifluoromethyl residue can change the amphiphilicity, the cross-sectional area, and, as a consequence, the permeability coefficient of a molecule.

Biological situation

The pH close to the surface of a living cell is generally acidic despite the fact that the extracellular lipid leaflet is electrically neutral. If one takes into account an acidic pH and the correspondingly low air–water partition coefficient (cf. Figure 2A) permeability coefficients can be orders of magnitude lower than those given in Table 2.

Even compounds with low permeability coefficients can in principle cross a membrane, provided the time to reach equilibrium is given. In natural environments however, equilibration time is limited by metabolic processes—for example, the action of cytochrome P450 and ATP-driven efflux transporters, such as P-glycoprotein, which bind molecules within the lipid membrane and export them out of the cell. If the export rate

of a drug is faster than the rate of passive diffusion into the cell (influx), the drug will barely reach the cytosol. However, if passive influx is distinctly faster than active efflux, the drug will reach the cytosol even if it is a substrate for an efflux transporter.^[14] The simple permeability predictions on the basis of SAMs provide an estimate of rates of passive influx of drugs and allow for comparison with the rates of efflux processes.^[14] The present approach opens new possibilities for a detailed understanding of membrane permeation in biological systems.

Keywords: chlorine · fluorine · ionization constants · kinetics · thermodynamics

- [1] A. Seelig, J. Seelig in *Encyclopedia of Physical Science and Technology*, 3rd ed. (Ed.: R. A. Meyers), Academic Press, N.Y., **2002**.
- [2] J. Seelig, A. Seelig, *Q. Rev. Biophys.* **1980**, *13*, 19.
- [3] D. Marsh, *Biochim. Biophys. Acta* **1996**, *1286*, 183.
- [4] A. Seelig, *Biochim. Biophys. Acta* **1987**, *899*, 196.
- [5] A. Seelig, *Biochemistry*. **1992**, *31*, 2897.
- [6] R. A. Demel, W. S. Geurts van Kessel, R. F. Zwaal, B. Roelofsen, L. L. van Deenen, *Biochim. Biophys. Acta* **1975**, *406*, 97.
- [7] V. Boguslavsky, M. Rebecchi, A. J. Morris, D. Y. Jhon, S. G. Rhee, S. Mclaughlin, *Biochemistry*. **1994**, *33*, 3032.
- [8] F. Hanakam, G. Gerisch, S. Lotz, T. Alt, A. Seelig, *Biochemistry*. **1996**, *35*, 11036.
- [9] H. Fischer, R. Gottschlich, A. Seelig, *J. Membr. Biol.* **1998**, *165*, 201.
- [10] X. Li-Blatter, E. Gatlik-Landwojtowicz, A. Seelig, unpublished results.
- [11] F. A. Gobas, J. M. Lahittete, G. Garofalo, W. Y. Shiu, D. Mackay, *J. Pharm. Sci.* **1988**, *77*, 265.
- [12] R. Bergmann, V. Eiermann, R. Gericke, *J. Med. Chem.* **1990**, *33*, 2759.
- [13] A. Seelig, R. Gottschlich, R. M. Devant, *Proc. Natl. Acad. Sci. USA* **1994**, *91*, 68.
- [14] A. Seelig, E. Gatlik-Landwojtowicz, *Mini-Rev. Med. Chem.* **2004**, in press.
- [15] P. Fromherz, *Rev. Sci. Instrum.* **1975**, *46*, 1380.
- [16] E. Gatlik-Landwojtowicz, X. Li-Blatter, A. Seelig, unpublished results.
- [17] M. R. Wenk, J. Seelig, *Biophys. J.* **1997**, *73*, 2565.
- [18] J. Seelig, S. Nebel, P. Ganz, C. Bruns, *Biochemistry*. **1993**, *32*, 9714.
- [19] S. Mclaughlin, *Annu. Rev. Biophys. Biophys. Chem.* **1989**, *18*, 113.
- [20] S. Mclaughlin, *Curr. Top. Membr. Transp.* **1977**, *9*, 71.
- [21] H. Fischer, M. Kansy, D. Bur, *Chimia* **2000**, *54*, 640.
- [22] J. E. True, T. D. Thomas, R. W. Winter, G. L. Gard, *Inorg. Chem.* **2003**, *42*, 4437.
- [23] R. F. Cookson, *Chem. Rev.* **1974**, *74*, 5.
- [24] A. Seelig, *Biochim. Biophys. Acta* **1990**, *1030*, 111.
- [25] K. Kitamura, S. Takegami, T. Kobayashi, K. Makihara, C. Kotani, T. Kitade, M. Moriguchi, Y. Inoue, T. Hashimoto, M. Takeuchi, *Biochim. Biophys. Acta* **2004**, in press.
- [26] S. Takegami, K. Kitamura, T. Kitade, A. Kitagawa, K. Kawamura, *Chem. Pharm. Bull. (Tokyo)*. **2003**, *51*, 1056.
- [27] P. Seiler, *Eur. J. Med. Chem.* **1974**, *9*, 473.
- [28] F. H. Clarke, *J. Pharm. Sci.* **1984**, *73*, 226.
- [29] U. Franke, A. Munk, M. Wiese, *J. Pharm. Sci.* **1999**, *88*, 89.
- [30] R. Mannhold, K. P. Dross, R. F. Rekker, *Quant. Struct-Act. Relat.* **1990**, *9*, 21.
- [31] D. W. Newton, R. B. Kluza, *Drug Intell. Clin. Pharm.* **1978**, *12*, 546.
- [32] F. H. Clarke, N. M. Cahoon, *J. Pharm. Sci.* **1987**, *76*, 611.
- [33] J. P. Tollenaere, H. Moereels, M. H. J. Koch, *Eur. J. Med. Chem.* **1977**, *12*, 199.

Received: January 20, 2004 [F 400017]